Spectrochimica Acta Part A 90 (2012) 202–207

Contents lists available at SciVerse ScienceDirect

Spectrochimica Acta Part A: Molecular and Biomolecular Spectroscopy

journal homepage: www.elsevier.com/locate/saa

K, Ca complexes with a sulfonic ligand: Structure and DNA-binding properties

Jiahe Luo[a], Zhaorong Ma[b], Huang Liang[b], Jiwen Chen[a], Zhengzhi Zeng[b,*]

[a] National Quality Supervision and Test Center for Paints, Guangdong Testing Institute for Product Quality Supervision, PR China
[b] Key Laboratory of Nonferrous Metals Chemistry and Resources Utilization of Gansu Province, State Key Laboratory of Applied Organic Chemistry and College of Chemistry and Chemical Engineering, Lanzhou University, Lanzhou 730000, PR China

ARTICLE INFO

Article history:
Received 5 August 2011
Received in revised form 8 January 2012
Accepted 16 January 2012

Keywords:
(E)-4-(2,4-dihydroxybenzylideneamino)benzenesulfonic acid
K and Ca complexes
Crystal structure
DNA binding
Photocleavage

ABSTRACT

A novel 4-(2,4-dihydroxybenzylideneamino)benzenesulfonic acid (HL), and its kalium(I), calcium(II) complexes $[M(L)n]\cdot 2nH_2O\cdot Cl_n$ (M = K(**1**) $n = 1$, M = Ca(**2**) $n = 2$), have been prepared and characterized. The crystal and molecular structures of **1** and **2** were determined by single-crystal X-ray diffraction. The interaction of **1**, **2** and ligand (**L**) with calf thymus DNA was investigated by UV–visible (UV–vis), fluorescence and viscosity measurements. Experimental results indicate that **1**, 2 and **L** could bind to DNA via the intercalation mode, and the binding affinity of **1** is stronger than that of **2** and **L**. The intrinsic binding constants of **1**, **2** and **L** were 5.60×10^5, 6.53×10^5 and 1.44×10^5 M^{-1}, respectively. The cleavage reaction on plasmid DNA has been monitored by agarose gel electrophoresis. The results indicated that **1** and **2** could cleave pBR322 DNA.

1. Introduction

Binding studies of metal complexes have become a very important field in the development of DNA molecule probes and chemotherapeutics in recent years [1–6]. In order to find anticarcinogens that can recognize DNA, people synthesized and developed many kinds of complexes. Among these complexes, metals or ligands can be varied in an easily controlled way to facilitate the individual applications [7–9]. A variety of small molecules can bind with DNA by electrostatic interaction with the exterior sugar—phosphate back-bone or by hydrophobic interaction along the minor groove of DNA or by intercalative interaction between the stacked bases pairs of native DNA from the major groove [10,11]. Among these factors governing the binding modes, it appears that the most significant is the molecular shape. Those complexes which best fit against the DNA helical structure display the highest binding affinity. Many useful applications of these complexes require that the complex bind to DNA through an intercalative mode, and the ligand intercalating into the adjacent base pairs of DNA. At present, a lot of complexes have been synthesized and their interactions with DNA were studied, and many of studies just focused on Transition-metal compounds. K, Ca are important element of life, and much research of them is about their effect on the growth of cells [12–14]. However, DNA-binding investigations of their complexes have been relatively few.

Compared with the number of studies dealing with mononuclear complexes, relatively few studies on binuclear and polynuclear complexes have been reported to date. The efficient enhancement of DNA cleavage activity for binuclear complexes [15–17] stimulates us to design and synthesize new binuclear complexes to evaluate and understand the factors on the DNA-binding properties. A familiar strategy to design and synthesize discrete polynuclear complexes is the use of the sulfonic ligand to react with metal salts. Sulfonated polymers have been found playing a very important role in the conventional proton conductive membranes manufacturing and electrochemical sensors based on DNA recognition. The complexes of it also developed very well in the dye, plating, and catalyser industry [18–21]. However, up to now, the biological activities and interactions with DNA of them and their complexes have not been explored.

These facts encouraged us to synthesize a new ligand, (E)-4-(2, 4-dihydroxybenzylideneamino)benzenesulfonic acid, and its alkali, alkaline earth metal complexes. Then, we evaluate the binding behaviors of these compounds with calf thymusDNA (CT-DNA), and explore their properties of cleaving Plasmid DNA.

Abbreviations: DMF, N,N-dimethyl formamide; UV–Vis, UV–visible; CT-DNA, calf thymus DNA; Tris, tris(hydroxymethyl) aminomethane; TMS, tetramethylsilane; FAB, fast-atom bombardment; EB, ethidium bromide.

* Corresponding author. Tel.: +86 931 8610877; fax: +86 931 8912582.
E-mail address: zengzhzh@yahoo.com.cn (Z. Zeng).

1386-1425/$ – see front matter © 2012 Elsevier B.V. All rights reserved.
doi:10.1016/j.saa.2012.01.035

2. Experimental

2.1. Materials and instrumentation

All reagents and solvents were purchased commercially and used without further purification unless otherwise noted. CT-DNA and pBR322 DNA were obtained from Sigma Chemicals Co. (USA). Agarose was purchased from Promega Co. (German), ethidium bromide (EB) were obtained from Huamei Chemical Co. (Beijing, China). The concentration of DNA was determined spectrophotometrically using a molar absorptivity of 6600 M^{-1} cm^{-1} (260 nm) [22].

The melting points of the compounds were determined on a Beijing XT4-100 microscopic melting point apparatus (the thermometer was not corrected). Carbon, hydrogen, and nitrogen were analyzed on an Elemental Vario EL analyzer. Infrared spectra (4000–400 cm^{-1}) were determined with KBr disks on a Therrno Mattson FTIR spectrometer. The UV–Vis spectra were recorded on a Varian Cary 100 UV–Vis spectrophotometer. The fluorescence spectra were recorded on a Hitachi RF-4500 spectrofluorophotometer. ^{1}H NMR spectra were measured on a Varian VR 300-MHz spectrometer, using TMS as a reference. Mass spectra were performed on a VG ZAB-HS Fast-atom bombardment (FAB) instrument and electrospray mass spectra (ESI-MS) were recorded on a LQC system (Finngan MAT, USA) using DMF as mobile phase.

2.2. Preparation of the ligand (**L**)

An ethanol solution containing 2,4-dihydroxybenzaldehyde (1.38 g, 10 mmol) was added dropwise to a suspension of 4-aminobenzenesulfonic acid (1.73 g, 10 mmol) in water (150 ml). The mixture was stirred and heated to reflux for 6 h. The yellow precipitate was collected by filtration and washed with ethanol. Recrystallistation from 1:1 (v/v) DMF/H_2O gave **L**, which was dried under vacuum. Yield, 85%. m.p. 209–211 °C. Elemental analysis: Found (calculated) (%) for $C_{13}H_{11}NO_5S$: C, 53.14 (53.24); H, 3.82 (3.75); N, 4.56 (4.78). ^{1}H NMR (DMSO-d_6 300 MHz, br, broad; s, singlet; m, multiplet): δ (ppm) 8.45 (1H, s, CH═N), 7.95–6.62 (7H, m, Ph—H). FAB MS: m/z = 294 (M+H). IR: ν_{max} (cm^{-1}): ν(C═N): 1631 cm^{-1}, $\nu(SO_3^-)$: 1388 cm^{-1}, 1232 cm^{-1}, ν(—OH): 3058 cm^{-1}.

2.3. Preparations of the complexes

A solution of ligand (0.29 g, 1.0 mmol) and NaOH (0.04 g, 1.0 mmol) in 1:1 (v/v) H_2O/CH_3CH_2OH (8 ml) was stirred at room temperature for 15 min. Then the mixture was heated to reflux for 6 h after added a solution of KCl (0.150 g, 2.0 mmol) in water (1 ml) to it. A red precipitate, the K(I) complex **1**, was separated from the solution by suction filtration, purified by washing several times with water and ether, and dried for 24 h under vacuum, yield 45%. The Ca(II) complex **2** was prepared by the same method, yield 58%. Elemental Analysis: Found (calculated) (%) for **1** $C_{13}H_{14}NO_7SK$ (%): C, 41.54 (41.60); H, 3.19 (3.16); N, 9.74 (9.69). IR for **1** (cm^{-1}): ν(C═N): 1631 cm^{-1}, $\nu(SO_3^-)$: 1329 cm^{-1}, 1197 cm^{-1}, ν(—OH): 3421 cm^{-1}. ES-MS [DMF, m/z]: 1470.45 (M+H); Elemental analysis. Found (calculated) for **2** $C_{52}H_{56}N_4O_{28}S_4Ca_2$ (%): C, 44.67 (44.78); H, 4.22 (4.02); N, 4.01 (4.02). IR for complex **2** (cm^{-1}): ν(C═N): 1631 cm^{-1}, $\nu(SO_3^-)$: 1345 cm^{-1}, 1223 cm^{-1}, ν(—OH): 3419 cm^{-1}. ES-MS [DMF, m/z]: 1358.2.

2.4. Crystallography

Table 1 summarizes the crystal data, data collection and refinement parameters for **1** and **2**. A light yellow crystal of **1** (0.26 mm × 0.23 mm × 0.23 mm) was selected for the X-diffraction analysis. Data collection was performed on a Rigaku RAXIS-RAPID diffractometer using a MoKα radiation (λ = 0.71073 Å) at 273(2) K. The intensity data were collected by the w scan mode within $1.94° < \theta < 25.5°$ for $h\,k\,l$ ($-9 \le h \le 9$, $-12 \le k \le 12$, $-21 \le l \le 16$) in the triclinic system. A light red crystal of **2** (0.27 mm × 0.23 mm × 0.21 mm) was also measured. Data were collected at 298(2) K using MoKa radiation (λ = 0.71073 Å). The intensity data were collected by the Omega scan mode within $1.15° < h < 25.00°$ for $h\,k\,l$ ($-18 \le h \le 21$, $-13 \le k \le 11$, $-17 \le l \le 17$) in the monoclinic system. The structure was solved by direct methods. The positions of non-hydrogen atoms were determined from successive Fourier syntheses. The hydrogen atoms were placed in their geometrically calculated positions. The positions and anisotropic thermal parameters of all non-hydrogen atoms were refined on F^2 by full-matrix least-squares techniques with the SHELX-97 program package (G.M. Sheldrick, Bruker AXS, Madison, WI, 2001) [23].

2.5. Spectroscopic studies on DNA interaction

2.5.1. Electronic absorption spectra

The UV–Vis absorbance at 260 and 280 nm of the CT-DNA solution in 50 mM NaCl/5 mM Tris–HCl buffer (pH 7.2) give a ratio of ~1.9, indicating that the DNA was sufficiently free of protein [24]. The DNA concentration was determined by measuring the UV absorption at 260 nm, taking the molar absorption coefficient (ε_{260}) of CT-DNA as 6600 M^{-1} cm^{-1} [22].

2.5.2. Fluorescence spectra

The complexes at a fixed concentration (10 μM) were titrated with increasing amounts of CT-DNA. Excitation wavelength of the samples were 338 nm, scan speed = 500 nm/min, slit width 10/10 nm. To compare quantitatively the affinity of the compound bound to DNA, the intrinsic binding constants K_b of the three compounds to DNA were obtained by the luminescence titration method. The concentration of the bound compound was calculated using the equation [25].

$$C_b = C_e \left[\frac{(F - F^0)}{(F^{max} - F^0)} \right]$$

where C_t is the total compound concentration, F is the observed fluorescence emission intensity at a given DNA concentration, F^0 is the intensity in the absence of DNA, and F^{max} is the fluorescence of the totally bound compound. Binding data were cast into the form of a Scathchard plot [26] of r/C_f versus r, where r is the binding ratio $C_b/[DNA]_t$ and C_f is the free ligand concentration. All experiments were conducted at 20 °C in a buffer containing 5 mM Tris–HCl (pH = 7.2) and 50 mM NaCl.

Further evidence for complexes **1** and **2**, and **L** binding to DNA via intercalation is given through the emission quenching experiment. EB is a common fluorescent probe for DNA structures and has been employed in examinations of the mode and process of metal complex binding to DNA [27]. A 2 mL solution of 10 μM DNA and 0.8 μM EB (at saturation binding levels) [28] were titrated by 0–6.5 μM complexes **1** and **2**, and 0–18 μM **L** (λ_{ex} = 500 nm, λ_{em} = 520.0–650.0 nm).

According to the classical Stern–Volmer equation [29].

$$\frac{F^0}{F} = K_q[Q] + 1$$

where F^0 is the emission intensity in the absence of quencher, F is the emission intensity in the presence of quencher, K_q is the quenching constant, and [Q] is the quencher concentration.

The shape of Stern–Volmer plots can be used to characterize the quenching as being predominantly dynamic or static. Plots of F^0/F versus [Q] appear to be linear and K_q depends on temperature.

Table 1
Crystal data and structure refinement for complexes **1** and **2**.

	1	**2**
Empirical formula	$C_{13}H_{14}NO_7SK$	$C_{52}H_{56}N_4O_{28}S_4Ca_2$
Formula weight	367.41	1393.41
Temperature (K)	296(2)	293(2)
Wavelength (Å)	0.71073	0.71073
Crystal system	Triclinic	Monoclinic
space group	P-1	Pc
Unit cell dimensions		
a (Å)	8.191(4)	17.805(12)
b (Å)	10.534(5)	11.669(8)
c (Å)	17.808(8)	14.658(10)
α (°)	92.302(7)	90
β (°)	94.227(7)	94.277(10)
γ (°)	93.116(7)	90
Volume (Å)	1528.6(12)	3037(4)
Z	4	2
Calculated density (Mg/m^3)	1.596	1.524
Absorption coefficient (mm^{-1})	0.520	0.417
F(000)	760	1448
Crystal size (mm)	$0.26 \times 0.23 \times 0.22$	$0.27 \times 0.23 \times 0.21$
θ range for data collection (°)	1.94–25.50	1.15–25
Reflections collected/ unique	7944/5581 [R(int) = 0.0126]	14747/8764 [R(int) = 0.0211]
Completeness to theta = 25.50	98.2%	99.8%
Absorption correction	None	Semi-empirical from equivalents
Refinement method	Full-matrix least-squares on F^2	Full-matrix least-squares on F^2
Data/restraints/parameters	5581/8/451	8764/2/813
Goodness-of-fit on F^2	0.891	1.076
Final R indices [I>2sigma(I)]	R1 = 0.0388 wR2 = 0.1181	R1 = 0.0472 wR2 = 0.1106
R indices (all data)	R1 = 0.0477 wR2 = 0.1301	R1 = 0.0528 wR2 = 0.1163
Largest diff. peak and hole ($eÅ^{-3}$)	0.416 and −0.401	1.033 and −0.380
CCDC number	754890	754891

2.5.3. Viscosity measurements

Viscosity experiments were conducted on an Ubbelodhe viscometer, immersed in a thermostated water-bath maintained at 25.0 ± 0.1 °C. Titrations were performed for the complexes (1–10 μM), and each compound was introduced into the CT-DNA solution (10 μM) present in the viscometer. Data were presented as $(\eta/\eta_0)^{1/3}$ versus the ratio of the concentration of the compound to CT-DNA, where g is the viscosity of CT-DNA in the presence of the compound and η_0 is the viscosity of CT-DNA alone. Viscosity values were calculated from the observed flow time of CT-DNA containing solutions corrected from the flow time of buffer alone (t_0), $\eta = t - t_0$ [30].

3. Results and discussion

3.1. X-ray structural characterization

1 and **2** were crystallized in the Triclinic and Monoclinic system, respectively. The structures of $[K_4L_4(H_2O)_8]$ (**1**) and $[Ca_2\ L_4(H_2O)_6]\cdot(H_2O)_2$ (**2**) are shown in Figs. 1 and 2, together with atom numbering scheme. In the complex **1**, the K(1)—O(3) and K(1)—O(9) sulfonic distances were 2.738(2) and 2.763(2) Å, respectively, while the K(1)—O(12) and K(1)—O(11) water distances were found to be 2.733(3) and 2.762(3) Å, respectively. The K(1)—K(2)#1 distance of 4.0029(18) Å clearly demonstrates

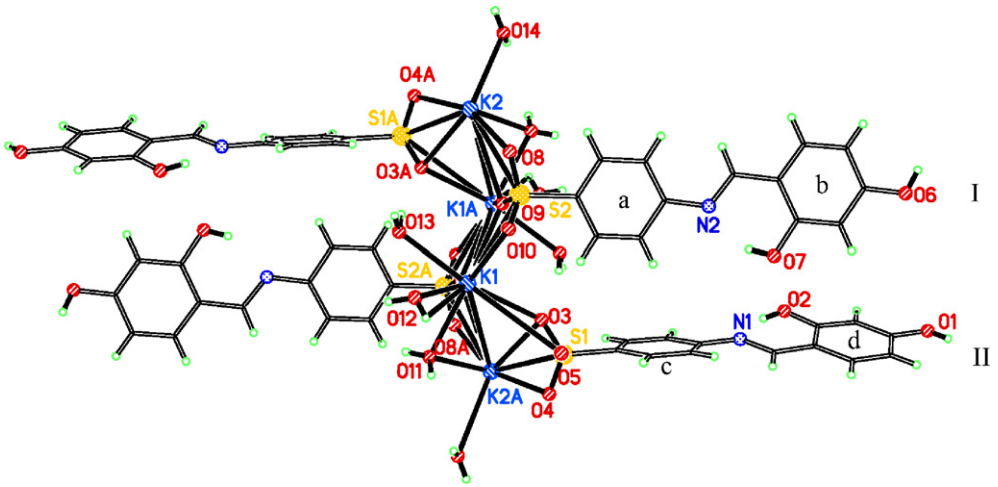

Fig. 1. The structure of complex **1**.

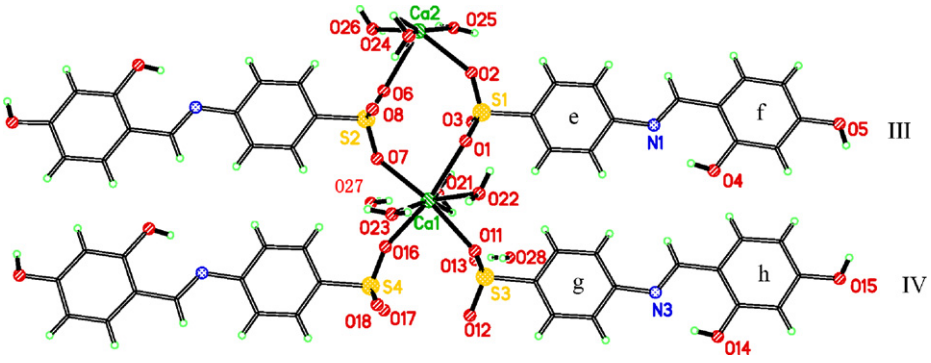

Fig. 2. The structure of complex **2**.

the weak metal–metal interaction, and is comparative to the metal–metal distance in $[(Ph_3P)Pt(u\text{-}bzta)_2RhCl(CO)]$(Pt–Rh 2.6266 Å) and $[Rh_4(u\text{-}HBzimt)_2Cl_2(CO)_8]$ (Rh–Rh 2.984 Å), in these cases the metals are bridged by bzta [31,32]. The torsion angle between the benzene rings a and b is 5.84°, which indicates that the ligand *I* is almost planar. The dihedral angle between *c* and *d* is 16.81°. The plane of benzene ring *a* is almost perpendicular to that of the *c*, as indicated by the torsion angle of them is 87.15°. In the complex **2**, the Ca(1)—O(7) and Ca(1)—O(1) sulfonic interactions were found to be 2.392(3) and 2.436(3) Å, respectively, the water distances were found to be 2.517(3) and 2.501(4) for Ca(1)—O(22) and Ca(1)—O(21). The ligand III and IV are nearly planar with the benzene rings e and f, g and h torsion angles of 4.23° and 6.39°, respectively. The dihedral angles between e and g, f and h are 3.69° and 5.87°, indicating the ligand III and IV are nearly parallel. The unit cell of **1**, **2** contains four and tow molecules, respectively (Figs. S1 and S2 in support information).

3.2. Infrared spectra

The IR spectra of the complexes are similar. The band at the 3058 cm^{-1} is ν(—OH) vibration in the ligand. In the complexes these bands are presented at 3421 and 3419 cm^{-1}, $\Delta\nu_{(ligand\text{-}complexes)}$ is to 363 and 361 cm^{-1}. These show that the complexes link some water molecules, and the peak of —OH is included by the peak of water. The $\nu(SO_3^-)$ vibration of the free ligand is at 1388 cm^{-1}, 1232 cm^{-1}, respectively; for the complexes these peaks shift to 1329, 1197 and 1345, 1223 cm^{-1}, $\Delta\nu_{(ligand\text{-}complexes)}$ is equal to 59, 35 and 43, 9 cm^{-1}. These data indicate that the oxygen of the sulfonic have formed a coordination bond with the metal ion which is consist with the X-ray structural. The band at 553 cm^{-1} for both **1** and **2** are assigned to ν(M–O), at 523 cm^{-1} for **1** is assigned to (M–S) [33]. These shifts demonstrate that the ligand coordinated Ca^{2+} and K^+ ions through the oxygen of sulfonic.

3.3. DNA-binding studies

3.3.1. Electronic absorption titration

The electronic absorption spectroscopy is one of the most important techniques for complexes binding with DNA [34]. The absorption spectra of **1**, **2** and **L** in the absence or presence of CT-DNA are given in Fig. 3. In the presence of CT-DNA, the absorption bands of **1**, **2** at 252 nm exhibited hypochromism of about 56.92%, 50.95%, respectively, and the free ligand at 254 nm exhibited hypochromism of about 13.21%. In the UV region, the intense absorption bands around 252 and 292 nm exist in title complexes, due to intraligand π–π^* transition of the coordinated groups. Addition of increasing amounts of CT-DNA resulted in a reduction in absorbency and slight red shift in the UV spectra of the title complexes and ligand. This phenomenon is attributed to the strong stacking interaction between aromatic group and the base pairs of CT-DNA, when **1**, **2** and **L** intercalate to the CT-DNA. **1** and **2** show somewhat more hypochromicity than **L**, indicating that the binding strength of **1** and **2** are much stronger than that of the free ligand.

3.3.2. Fluorescence spectra

In the absence of DNA, **1**, **2** and **L** can emit luminescence in Tris buffer at ambient temperature, with a maximum appearing at 453 nm for them. As shown in Fig. S3 (support information), the fluorescence intensities of the compounds are quenched steadily with the increasing concentration of the CT-DNA. The binding of **1**, **2**, and **L** to CT-DNA leads to a marked increase in the emission intensity, which also agrees with those observed for other intercalators [35]. According to the Scathchard equation, a plot of r/C_f versus r gave the binding constants of 5.60×10^5, 6.53×10^5 and 1.44×10^5 m^{-1} from the fluorescence data for **1**, **2** and **L**, respectively. These results show that the complexes bind more strongly than the free ligand. The higher binding affinity of the Ca^{2+}, K^+ complexes are attributed to the extension of the π system of the intercalated ligand due to the coordination of the alkali and alkaline-earth metals.

The emission spectrum of EtBr bind to DNA in the absence or presence of the **1**, **2** and **L** is given in Fig. S4 (support information). The emission intensity of the DNA–EB system (λ_{em} = 594 nm) decreased apparently as the concentration of **1**, **2** and **L** increased. An isobathic point appeared at 552 nm, which indicated the formation of a complex-DNA system. These changes show that **1**, **2** and **L** replaced EB from the DNA–EB system, leading to the decreased emission of the DNA–EB system. The quenching plots illustrate that the quenching of EB bound to DNA by the complexes is in good agreement with the linear Stern–Volmer equation. In the plots of F^0/F versus [Q], K_q is given by the ratio of the slope to the intercept. The K_q values for **1**, **2** and **L** are 5.54×10^5, 1.77×10^5 and 7.90×10^3 M^{-1}, respectively. Since these changes indicate only one kind of quenching process, it may be concluded that **1**, **2** and **L** bind to CT-DNA via the same mode (intercalation mode) [36].

3.3.3. Viscosity study

Hydrodynamic methods such as viscosity, which are exquisitely sensitive to the length change of DNA, may be the most effective means studying the binding mode of complexes to DNA in the absence of X-ray crystallographic or NMR structural data [26]. A classical intercalation model results in the lengthening of the DNA helix as base pairs become separated to accommodate the binding ligand, thus leading to an increase of CT-DNA viscosity. In contrast, a partial and/or non-classical intercalation of ligand could bend (or kink) the DNA helix, reducing its effective length and, concomitantly, its viscosity [37]. The effects of **1**, **2** and **L** on the viscosity of CT-DNA at 25.0 °C are shown in Fig. 4. The viscosities of the DNA increased steadily with increasing concentrations of **1**, **2** and **L**. The

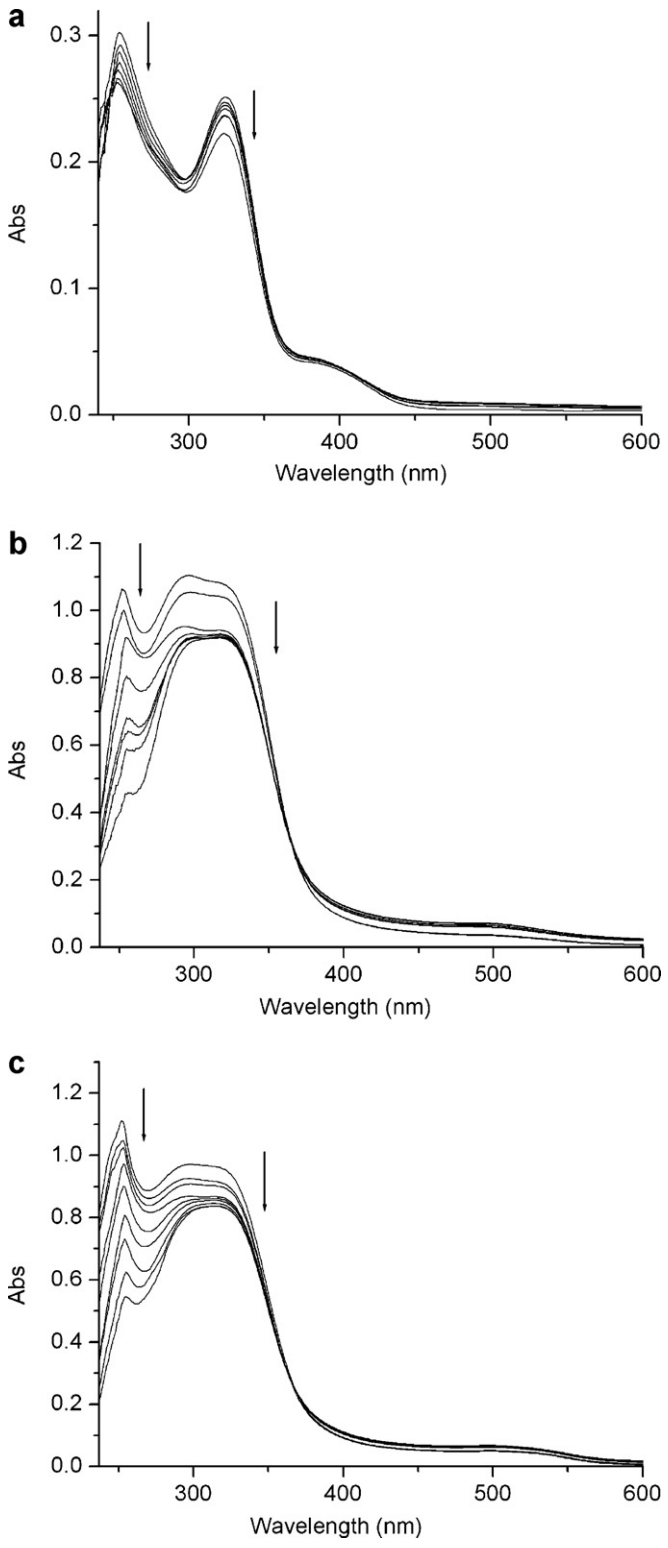

Fig. 3. (a) Electronic spectra of ligand (10 uM) in the presence of increasing amounts of CT-DNA. [DNA] = 0–20 μM. The arrow indicates the absorbance changes upon increasing DNA concentration (the concentration of DNA is expressed per nucleotide). (b) Electronic spectra of K complex (10 μM) in the presence of increasing amounts of CTDNA. [DNA] = 0–40 μM. The arrow indicates the absorbance changes upon increasing DNA concentration. (c) Electronic spectra of Ca complex (10 μM) in the presence of increasing amounts of CT-DNA. [DNA] = 0–30 μM. The arrow indicates the absorbance changes upon increasing DNA concentration.

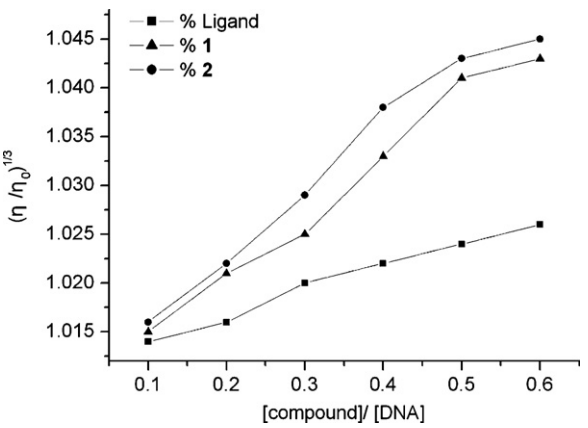

Fig. 4. Effect of increasing amounts of the compounds on the relative viscosity of CT-DNA at 25.0 ± 0.1 °C.

results clearly show that both the compounds and **L** can intercalate between adjacent DNA base pairs, causing an extension in the helix, and thus increase the viscosity of DNA, and the complexes can intercalate more strongly and deeply than the free ligand. The results obtained from viscosity studies validate those obtained from the spectroscopic studies.

3.3.4. Electrophoretic analysis

The cleavage reaction on plasmid DNA can be monitored by agarose gel electrophoresis. When circular plasmid DNA is subject to electrophoresis, relatively fast migration will be observed for the intact supercoil form (Form I, CCC form). If scission occurs on one strand (nicking), the supercoiled will relax to generate a slower-moving open circular form (Form II, OC form). If both strands are cleaved, a linear form (Form III) that migrates between Form I and Form II will be generated. As shown in Fig. S5 (support information), the results indicate that the CCC form of pBR322 DNA diminishes gradually, whereas the Form II (OC) form increases with the increase of concentration of **1**, **2** gradually. No DNA cleavage was observed for controls in which the complexes were absent (lane 0). At the concentration of 80 μM, **1** and **2** can almost promote the complete conversion of DNA from Form I to Form II (lane 4). Therefore, the result here indicates that **1** and **2** can bind to and cleave DNA efficiently.

4. Conclusion

In summary, a novel (E)-4-(2,4-dihydroxybenzylideneamino) benzenesulfonic acid ligand (**L**) and its K, Ca complexes have been prepared and fully characterized. The crystal structures of the complexes were determined by single crystal X-ray diffraction. The DNA-binding properties of **1**, **2** and **L** were investigated by absorption, fluorescence and viscosity measurements. The results indicate that the compounds and the L bind to CT-DNA via intercalation. The binding constants show that the DNA binding affinity increases in the order **L** < **2** < **1**. The cleavage reaction on plasmid DNA has been investigated by agarose gel electrophoresis. Remarkably, the results indicate that the complexes exhibit an efficient DNA-cleavage function.

Acknowledgment

This project was supported by the National Natural Science Foundation in China (20171019).

Appendix A. Supplementary data

Supplementary data associated with this article can be found, in the online version, at doi:10.1016/j.saa.2012.01.035.

References

[1] P.J. Dardlier, R.E. Holmlin, J.K. Barton, Science 275 (1997) 1465–1468.
[2] D.B. Hall, R.E. Holmlin, J.K. Barton, Nature 382 (1996) 731–735.
[3] A.E. Friedman, J.C. Chamborn, J.P. Sauvage, N.J. Turro, J.K. Barton, J. Am. Chem. Soc. 114 (1992) 5919–5925.
[4] P. Lincoln, B. Norden, Chem. Commun. (1996) 2145–2146.
[5] R.M. Hartshorn, J.K. Barton, J. Am. Chem. Soc. 112 (1990) 4960–4962.
[6] N.B. Thornton, K.S. Schanze, Inorg. Chem. 32 (1993) 4994–4995.
[7] D.S. Sigman, A. Mazumder, D.M. Perrin, Chem. Rev. 93 (1993) 2295–2316.
[8] G. Pratvicl, J. Bernadou, B. Mcunicr, Adv. Inorg. Chem. 45 (1998) 251–312.
[9] L.N. Ji, X.H. Zou, J.G. Liu, Coord. Chem. Rev. 216 (2001) 513–536.
[10] G.M. Zhang, S.M. Shuang, C. Dong, D.S. Liu, M.M.F. Choi, J. Photochem. Photobiol. B 74 (2004) 127.
[11] C. Li, S.L. Liu, L.H. Guo, D.P. Chen, Electrochem. Commun. 7 (2005) 23.
[12] S. Haider, S. Khalid, S.J. Tucker, F.M. Ashcroft, M.P. Sansom, Biochemistry 46 (2007) 3643–3652.
[13] M. Haruta, G. Monshausen, S. Gilroy, M.R. Sussman, Biochemistry 47 (2008) 6311–6321.
[14] W. Namkung, P. Padmawar, A.D. Mills, A.S. Verkman, J. Am. Chem. Soc. 130 (2008) 7794–7795.
[15] M.C.B. Oliveira, M.S.R. Couto, P.C. Severino, T. Foppa, G.T.S. Martins, B. Szpoganicz, R.A. Peralta, A. Neves, H. Terenzi, Polyhedron 24 (2005) 495–499.
[16] K.G. Ragunathan, H.J. Schneider, Angew. Chem. Int. Ed. 35 (1996) 1219.
[17] E.J. Gao, K.H. Wang, X.F. Gu, Y. Yu, Y.G. Sun, W.Z. Zhang, H.X. Yin, Q. Wu, M.C. Zhu, X.M. Yan, J. Inorg. Biochem. 101 (2007) 1404–1409.
[18] M.L. Ponce, D. Gomes, S.P. Nunes, J. Membr. Sci. 319 (2008) 14–22.
[19] X.Q. Lin, G.F. Kang, L.P. Lu, Bioelectrochemistry 70 (2007) 235–244.
[20] Y.L. Li, S.F. Zhang, J.Z. Yang, S. Jiang, Q. Li, Dyes Pigments 76 (2008) 508–514.
[21] A. Panchaudly, E. Guillaume, M. Affolter, F. Robert, P. Moreillon, M. Kussmann, Rapid Commun. Mass Spectrom. 20 (2006) 1585–1594.
[22] P.X. Xi, Z.H. Xu, F.J. Chen, Z.Z. Zeng, X.W. Zhang, J. Inorg. Biochem. 103 (2009) 210–218.
[23] R.H. Blessing, Acta. Crystallogr. A: Found. Crystallogr. A51 (1995) 33–38.
[24] S. Satyanarayana, J.C. Dabrowiak, J.B. Chaires, Biochemical 32 (1993) 2573–2584.
[25] C.V. Kumar, E.H. Asuncion, J. Am. Chem. Soc. 115 (1993) 8547–8553.
[26] S. Satyanarayana, J.C. Dabrowiak, J.B. Chaires, Biochemistry 31 (1992) 9319–9324.
[27] M. Howe-Grant, K.C. Wu, W.R. Bauer, S. Lippard, J. Biochem. 19 (1976) 247–339.
[28] J.K. Barton, A. Danishefsky, J. Goldberg, J. Am. Chem. Soc. 106 (1984) 2172–2176.
[29] M.R. Eftink, C.A. Ghiron, Anal. Biochem. 114 (1981) 199–206.
[30] T.C. Michael, R. Marisol, J.B. Allen, J. Am. Chem. Soc. 111 (1989) 8901–8911.
[31] M.A. Ciriano, J.J. Pe′rez-Torrente, F.J. Laboz, L.A. Oro, Inorg. Chem. 31 (1992) 969–974.
[32] C. Tejel, B.E. Villarroya, M.A. Ciriano, A.J. Edwards, F.J. Lahoz, L.A. Oro, M. Lanfranchi, A. Tiripicchio, M. Tiripicchio-Camellini, Inorg. Chem. 37 (1998) 3954–3963.
[33] F.D. Lewis, S.V. Barancyk, J. Am. Chem. Soc. 111 (1989) 8653–8661.
[34] A. Nohara, T. Umetani, Y. Sanno, Tetrahydr. Lett. 22 (1973) 1995.
[35] B.D. Wang, Z.Y. Yang, P. Crewdson, D.Q. Wang, J. Inorg. Biochem. 101 (2007) 1492–1504.
[36] F.H. Li, G.H. Zhao, H.X. Wu, H. Lin, X.X. Wu, S.R. Zhu, H.K. Lin, J. Inorg. Biochem. 100 (2006) 36–43.
[37] C.Y. Zhou, J. Zhao, Y.B. Wu, C.X. Yin, P. Yang, J. Inorg. Biochem. 101 (2007) 10–18.